Environmental Pollution 288 (2021) 117752

Contents lists available at ScienceDirect

Environmental Pollution

journal homepage: www.elsevier.com/locate/envpol

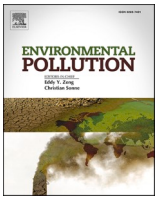

Mercury distribution in the East Himalayas: Elevational patterns in soils and non-volant small mammals☆

Yanju Ma [b,c], Lihai Shang [d], Huijian Hu [a], Wei Zhang [d,e], Lianghua Chen [c], Zhixin Zhou [a], Paras Bikram Singh [a], Yiming Hu [a,*]

[a] Guangdong Key Laboratory of Animal Conservation and Resource Utilization, Guangdong Public Laboratory of Wild Animal Conservation and Utilization, Institute of Zoology, Guangdong Academy of Sciences, China
[b] School of Environmental Science & Engineering, Southern University of Science and Technology, Shenzhen, Guangdong, 518005, China
[c] School of Economics and Management, Southeast University, Nanjing, Jiangsu, 210088, China
[d] State Key Laboratory of Environmental Geochemistry, Institute of Geochemistry, Chinese Academy of Sciences, Guiyang, 550081, China
[e] University of Chinese Academy of Sciences, Beijing, 100049, China

ARTICLE INFO

Keywords:
Himalayas
Mercury
Rodent
Accumulation
Biomonitoring
Hair

ABSTRACT

Mercury (Hg), as a global pollutant, its contamination has been documented in environmental compartments of the Himalayan region. However, little research exists regarding to Hg accumulation in terrestrial wildlife, as well as its driving factors. In this study, surface soil and small mammals were collected in the Lebu Valley, East Himalayas of China, in order to measure the uptake of the long-distance transported Hg along an elevational gradient approximately from 2300 to 5000 m a.s.l. The soil Hg concentrations were measured and predicted mostly by vegetation type as well as soil organic matter, while the Hg in hair of small mammals (Muridae and Cricetidae) showed deeply influenced by soil Hg. Notably, combined with the field survey data, soil and hair Hg were both enhanced in low and mid-elevations, which overlapped the distribution ranges of a majority of mammals. Overall, this indicates that Hg contamination in low- and mid-elevations poses a potential threat to the top predators that consuming small mammals directly or indirectly. Furthermore, our data advances the understanding of Hg dynamics in remote, high mountain ecosystems and provides baseline data for biomonitoring for reduction of Hg emission globally.

1. Introduction

The mountainous areas have traditionally been thought to be a pristine paradise for wildlife with limited human-driven disturbance. However, high-elevation regions were also considered as condensers for a variety of volatile and semi-volatile persistent toxic pollutants, which are emitted from increasing anthropogenic activities remotely and redeposited back to ecosystems through the "grasshopper effect" and "mountain cold-trapping effect" (Loewen et al., 2005; Wania and Mackay, 1995; Zhang et al., 2013). Among toxicants, mercury (Hg) has been recognized as a well-known, persistent and hazardous contaminant globally (Driscoll et al., 2013). Due to toxicities, trans-boundary and long-range air transportation abilities, as well as the capacities of bioaccumulation and biomagnification along food webs, Hg and its components, particularly methyl-mercury (MeHg), pose serious threats to wildlife and human (Chételat et al., 2020; Rice et al., 2014). The estimated atmospheric emission is mainly from combustion of fossil fuels and biomass, such as coal combustion and non-ferrous metal production. Furthermore, almost half of the emission occurs in Asia (UN Environment, 2019). Worse, unlike other remote ecosystems (e.g. the Polar region), the Himalayas, which is well-known as "the world's third pole", actually locates among large Hg emitted areas, i.e. East Asia, South Asia and Southeast Asia (Loewen et al., 2005). Meantime, its complicated geological topography, significant vertical climatic zonation with biological and environmental characteristics, together make this area one of the world's biodiversity hotspots (Myers et al., 2000). In fact, Hg content has been recorded in environmental compartments (e.g. water, soil and glacier) of the Himalayas (Sun et al., 2020; Tripathee et al., 2019; Wang et al., 2008). However, bioaccumulation in terrestrial mammals remains unclear. In such circumstances, if Hg contamination

☆ This paper has been recommended for acceptance by Professor Christian Sonne.

* Corresponding author.
E-mail address: yiming1226@126.com (Y. Hu).

https://doi.org/10.1016/j.envpol.2021.117752
Received 9 January 2021; Received in revised form 5 July 2021; Accepted 6 July 2021
Available online 16 July 2021

exists in the environment, whether and how organisms respond to this pollutant in the hotspot of global biodiversity, would be of significance to ecological conservation.

Small mammals are abundant and important components of terrestrial ecosystems, offering prey for other higher trophic predatory mammalian and avian species. Thus, with limited home range, small mammals, act as bioindicators to provide insights into local contaminant loading and accumulation in terrestrial ecosystems. Often, the commonly sampled species belong to three families of Soricidae (shrews), Cricetidae (hamsters and voles), and Muridae (Old World mice and rats) (Talmage and Walton, 1991). For instance, small mammals have been extensively used for the assessments of environmental contaminant exposure in mine tailings and industrial areas for effectively understanding contamination in wildlife (Gdula-Argasińska et al., 2004; Gerstenberger et al., 2006; Pankakoski et al., 1993; Turna Demir and Yavuz, 2020). During hair growth, Hg can be transported by circulating blood from internal tissues and incorporated into this keratin structure (Crewther et al., 1965). With less harming to individuals, hair Hg has been widely applied in the ecotoxicological field for biomonitoring in Europe and North America (e.g., Martinková et al., 2019; Peterson et al., 2021) and provide insights into local contamination.

Studies in terrestrial ecosystems indicate that Hg contamination varied along elevations. For instance, Hg accumulation showed an increasing trend along elevation (Blais et al., 2006; Townsend et al., 2014; Yu et al., 2011; Zhang et al., 2013), likely due to the "mountain-trapping effect" (Loewen et al., 2005; Wania and Mackay, 1995; Zhang et al., 2013). Moreover, vegetation type (Gerson et al., 2017; Obrist et al., 2017, 2012), vegetation photosynthetic activity (Fu et al., 2019), soil characteristics (Gerson et al., 2017), precipitation and temperature (Loewen et al., 2005) might contribute to Hg accumulation. However, knowledge regarding to the drivers that predict the bioaccumulation in terrestrial ecosystems at higher elevation (>2500 m a.s.l.) has been rarely tested (Ecke et al., 2020; Martinková et al., 2019), particularly along large elevational gradients.

In the highest mountainous ecosystem i.e. the Himalayas, the Hg contamination in small terrestrial mammals, and factors contributing to Hg accumulation, are sorely lacking. Moreover, elevational gradients of mountain ecosystems condense a large amount of environmental variation into a small geographical space, providing us ideal natural experiment systems for examination of Hg bioaccumulation. Making good use of the valley ecosystem as a natural laboratory with varied terrestrial landscapes across large elevational transects, we seek to assess Hg contamination in the East Himalayas. The specific objectives include below: 1) examine total Hg content and its trends in the environment (soil) and small mammals (rodent) along elevational gradient; 2) test the potential environmental drivers that predict Hg contamination: soil organic matter (SOM), vegetation type, local vegetation activity (the Normalized Difference Vegetation Index, hereafter NDVI), precipitation, temperate and/or soil Hg); 3) combined field survey data for mammal community, identify mammalian species at Hg risk in certain elevational ranges.

2. Methodology

2.1. Study area

Our field works were conducted in the Lebu Valley (26°25′ - 28°27′N, 91°28′ - 94°22′E), located in the East Himalayas of China (Fig. 1). There are five main vegetation zones across the 2700 m elevational gradience from 2300 to 5000 m a.s.l: broadleaf deciduous forest (2300–2900 m a.s.l.); coniferous and broadleaf mixed forest (2900–3500 m a.s.l.); dark coniferous forest (3500–3800 m a.s.l.); alpine shrub and meadows (3800–4400 m a.s.l.) and alpine meadow (4400–5000 m a.s.l.). Thus, the low elevation range (2300–3200 m a.s.l.) is dominated by deciduous forest type and its transited zone with coniferous; the mid-elevation range (3200–4100 m a.s.l.) consists of the transited zone and coniferous forests, while the high elevation (4100–5000 m a.s.l.) is in the range of alpine zone. Habitats are continuous along the elevational gradients and relatively undisturbed.

2.2. Mammal community investigation

From May 2018 to September 2019, non-volant mammals in our study area were surveyed using a standardized protocol by snap traps, camera traps, and visual observations along nine 300-m elevational bands from 2300 to 5000 m a.s.l. Field surveys could not be done at lower or higher elevations because of inaccessible topography (e.g., turbulent rivers and cliffs). Sampling was standardized to keep the same

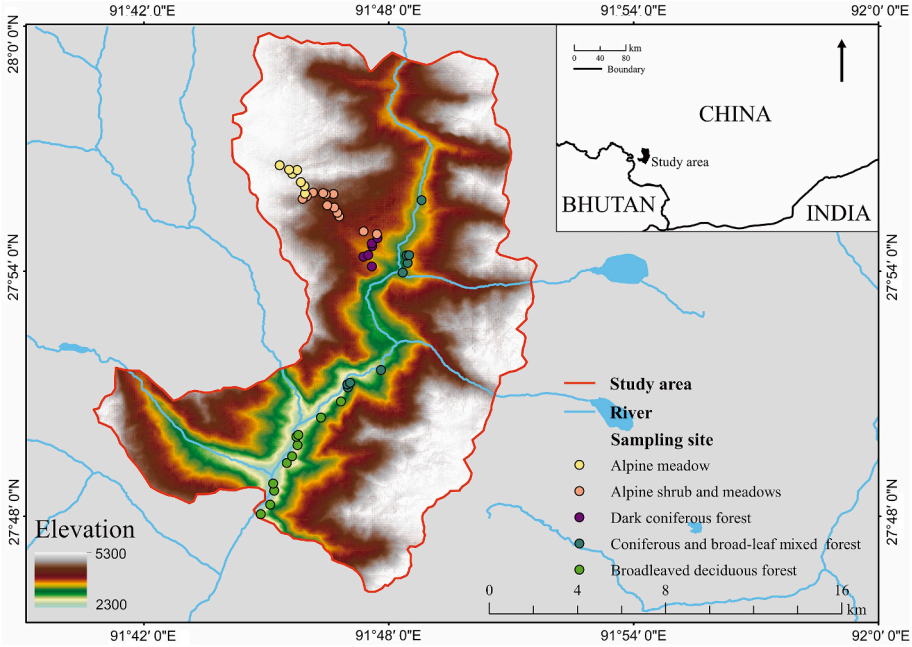

Fig. 1. Details of study site in the Lebu Valley, East Himalayas of China. Colored solid points present sampling site for various vegetated habitats.

sampling intensity across elevations.

2.2.1. Mammal investigation

We made two replicated surveys during the wet seasons (May to September): one in the early wet season (May to June) and the other in the late wet season (August to September), with the same sampling effort. There were five trapping sites for typical representative habitats in each elevational band (a total of 45 sites). Each trapping site included 30 snap traps (120 × 60 mm) that were placed 2–3 m apart. Trapping at each site was conducted for six consecutive nights for a total of 16,200 trap nights. To reduce the temporal autocorrelation among sites, elevational bands were sampled in a random order. Considering the different diets of non-volant mammals, the traps were baited with fried peanuts and ham (in equal proportions by weight). The traps were checked once a day in the morning and re-baited if needed. The captured individuals were identified, measured, and weighed.

Camera trap and visual observation were focused on medium and large-bodied mammals which could not be sampled by snap trap. The camera traps were established alongside the small mammal trapping sites (>30 days for each camera, a total of 45 camera traps were set along the elevational gradient). For the visual observation, we recorded and counted only the first visual observations of each mammal in the trapping site of each elevational band during our field survey, in each season, to avoid recording the same individual twice. Taxonomy of mammals followed Jiang et al. (2015). Bats (Chiroptera) were excluded from our statistical analyses, because it was difficult to sample the bat species adequately using our sampling protocol in the study area.

2.2.2. Species composition

In total, we recorded 27 mammal species (including 1 unknown species, *Niviventer. sp*) in our field surveys, including 8 carnivores, 2 primates, 6 artiodactyls, 8 rodents, 2 insectivores and 1 lagomorph (see Table S1). Since our goal is to better understand the primary consumers from the base of the food webs, we mainly chose herbivorous individuals (n = 68) from families Muridae and Cricetidae here to study Hg bioaccumulation. Specifically, Smoke-bellied Rat (*Niviventer eha* ranged from 2300 to 3800 m a.s.l.) and Stoliczka's Mountain Vole (*Alticola stoliczkanus* ranged from 3200 to 5000 m a.s.l.) were the most common small mammals with a relatively larger elevational range in the Lebu Valley.

We used species distribution and species richness to identify species distribution trends along elevation. The range of species distribution was identified as the difference between the lowest and highest elevations recorded for each species. We assumed that species potentially exist between its elevational limits. To avoid species being "lost" between sampling elevations, species with elevational ranges less than 300 m (or species with a single elevational distribution record, elevational range of 0 m were adjusted to 300 m considering the mobility of our studied taxa. Species richness of each 300-m elevational band was the number of species existed in the band.

2.3. Small mammal hair and soil sample collection

In 2019, for each elevational band, approximately 0.1 g hair from upper back of small mammal individuals was collected and put into paper coin envelopes or polyethylene bag. In addition, we collected five soil samples (10 cm from surface, ~20 g per sample) randomly using soil collectors in total 44 samples were collected and were packed into the plastic bag. All hair and soil samples were labeled clearly in location, vegetation type and time, then transported by car to the laboratory of the Institute of Zoology, Guangdong Academy of Sciences, then stored at cool ambient temperature until further analysis. Approval for capturing, handling and taking samples from small mammals was granted by the Forestry Bureau of Cuona County and Department of Forestry of Tibet Autonomous Region (the regulatory approval number: 2018–32).

2.4. Environmental data collection

To catch the precise characteristics of the meteorological condition, we placed mini weather stations in seven 300-m elevation transects (2440, 2822, 2914, 3311, 3499, 4219, and 4504 m a.s.l.) in the Lebu Valley. Each mini weather station included two data loggers (HoBo Pro-RH/Temp and HoBo Pro-Precipitation/Temp) and was surrounded by a mesh wire fence to keep interference from wild animals. Mean daily temperature (temperature) and amount of precipitation (precipitation) were measured and recorded between August 2018 and August 2019. Specifically, temperature data were recorded every 10 min and were averaged afterward 1 h to minimize the impact of possible outliers. Temperatures were extrapolated to all nine elevational bands using simple ordinary least squares regression. Precipitation data were extrapolated to all elevational bands in the study area using ArcGIS 10.4 (Oliver and Webster, 2007). Vegetation types were recorded during the field survey for each elevational band. In addition, the NDVI was used as a proxy for net primary productivity. We extracted NDVI data (1-km^2 resolution) in each 300-m elevational band of January, April, July and October for 4 consecutive years (2009–2012) from the Computer Network Information Center, Chinese Academy of Sciences (date of the download: 2016/6/17).

2.5. Mercury determination

Prior to Hg analysis, soil samples were dried at 40 °C overnight, manually ground, and sieved through a 75 μm mesh to remove large debris, while hair samples were washed by 90% acetone, then rinsed by D.I. water and dried at 40 °C. We analyzed the soil and hair samples for total Hg (THg) concentration using a Direct Mercury Analyzer (DMA 80, Milestone Inc., Italy) at wavelength used of 253.7 nm, following US Environmental Protection Agency Method 7473 (U.S. Environmental Protection Agency, 2000) at the State Key Laboratory of Environmental Geochemistry. The certified reference materials DORM-4 (fish protein, National Research Council Canada) and GSS-5 (soil, National Research Center for Standards in China) to confirm that this approach ensured complete combustion of the sample and did not contribute measurable contamination. Laboratory quality control samples included system and method blanks, calibration check standard, and a duplicate sample with each batch of 10 or fewer samples. The method detection limit for the DMA 80 is 0.0008 μg/g dry weight. Relative percentage differences (mean ± sd) for duplicate samples were 10.61 ± 9.51% (n = 9). Recoveries of GSS-5 was 100 ± 2.66% (n = 5), while DORM-4 was 97 ± 3.15% (n = 3). All Hg analyses met the measurement quality objectives in accordance with the certified methods.

2.6. SOM determination

Approximately 0.5 g dried samples for SOM were determined following a national standard method (GB 9834–88, a modified version from Nelson and Sommers, 1996). The procedure involves using $K_2Cr_2O_7$ ($Cr_2O_7^{2-}$) to oxidize soil organic carbon (SOC), and $FeSO_4$ to reduce the excess $Cr_2O_7^{2-}$ in solution. The amount of $Cr_2O_7^{2-}$ consumed in the reaction is used to estimate the carbon content of the soil, and times 1.724 to convert to SOM. The duplicate measurements were performed, and the relative standard deviations of sample duplicates were all below 5%.

2.7. Statistical analysis

Polynomial regression analyses were performed to assess the form of the patterns of species richness and THg (both in soil and small mammals) as a function of elevation along the gradient. Order 1 equation indicates linear pattern, whereas order 2 and order 3 equations indicate unimodal pattern (hump-shaped pattern). Further, we applied the Kruskal-Wallis test to find out the differences of THg accumulation

among low, medium and high elevation ranges. To determine factors contributing to variation in soil THg, we conducted a series of linear regression models to examine the effects of potential environmental variables, including vegetation, NDVI, SOM, precipitation and temperature in candidate models.

We then evaluated the effects of these environmental factors, as well as soil THg in small mammalian species in another set of candidate linear regression models. We used an information theoretic approach, which builds on likelihood estimates and yields an assessment of a collection of models to select the most parsimonious model, separately (Burnham et al., 2011). We used the second order Akaike information criterion (AIC*c*), a version of Akaike's Information Criteria (AIC) corrected for a small sample size, with an extra penalty term for the number of parameters. In fact, AICc is one of the commonly used metrics for model evaluation and selection for prediction error and model robustness. Also, ΔAIC*c*, the difference between a model's AIC*c* value and that of the best-supported model in the candidate set, was applied to select the top models (Symonds and Moussalli, 2011). Support for each model was evaluated using the Akaike weight (w_i), which represents the relative likelihood of the model, given the data, relative to all other models in the candidate set. Variable importance weights were used to assess an individual variable's relative importance within the candidate model set. Notably, the autocorrelation of environmental factors could affect the credibility of the results; thus, autocorrelation analysis was performed prior to model running. The variables with autocorrelation were avoided put together in candidate models (See Table S2).

Soil and hair THg were both reported as mean ± s.d. μg/kg dry weight and were natural log transformed to improve the assumption of normality and fitted linear trend lines for statistical analysis. Data were checked visually for normality and residuals of all models were assessed for normality using diagnostic plots and qq-plots. We performed linear models and model selection analysis in R version 3.6.0 using the Package "MuMIn" (version 1.43.15, Bartoń, 2019).

3. Results and discussion

3.1. Elevational pattern of mercury distribution and its conservation implication

Overall, the elevational range in our study area is among the largest ranged and the highest altitude reported elevational research in Hg contamination (Blackwell & Driscoll, 2015; Townsend et al., 2014; Tripathee et al., 2019; Wang et al., 2008), providing further data to understand Hg bioaccumulation in high mountain terrestrial ecosystems. Specifically, the average of surface soil THg in the Lebu Valley is 54.8 ± 31.2 μg/kg (ranged: 10.69 μg/kg in the alpine meadow zone to 112.23 μg/kg in the transition zone, Fig. 2, n = 44). The soil THg is comparable to the background values of the world soils, and it actually consists with the soil Hg reported in the Central Himalaya, Nepal (Tripathee et al., 2019). The mean of small mammalian THg is 43.0 ± 35.0 μg/kg range from 8.25 to 183.0 μg/kg (Fig. 2; n = 68). The Hg content in hair of small rodents feeding on primary herbivorous diets is comparable or even higher to Hg reported in some mammals collected at locations with active human disturbance (Huckabee et al., 1972), such as the Las Vegas Valley (Gerstenberger et al., 2006).

We observed a unique Hg trend in the floor and its subsequent bioaccumulation in primary consumers from the highest elevational terrestrial ecosystems. The enhanced Hg in the low and mid-elevations did not follow the general trend of Hg contamination in mountainous landscapes. For instance, Blackwell and Driscoll (2015) observed that a continuously increasing pattern in Hg deposition from the deciduous to alpine zone along the Whiteface Mountain, so did other montane studies (Stankwitz et al., 2012; Townsend et al., 2014; Zhang et al., 2013). Unlike the increasing pattern of Hg contamination in environmental compartments (e.g. atmospheric Hg inputs and ice core), in our case, the polynomial regressions for THg along elevations in the Lebu Valley

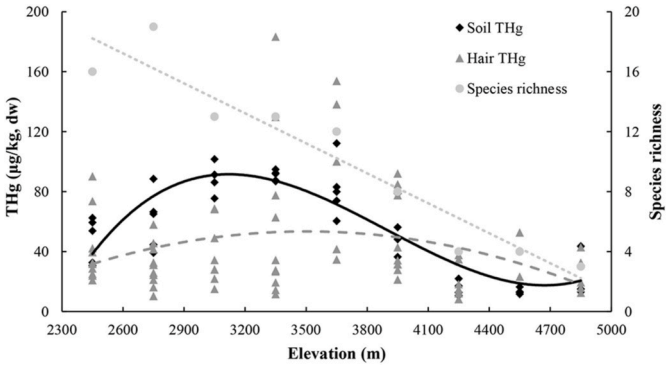

Fig. 2. Hair THg and top soil THg concentrations, mammal species richness along elevational gradience in the Lebu Valley, East Himalayan Mountain, China. Black diamonds represent data points from soil THg, grey triangles present data points from hair THg, and light grey dots present data points from mammal species richness. Lines are the patterns predicted by the best polynomial regression for soil THg (blackline, order 3), hair THg (grey dashed line, order 2) and mammal species richness (light grey dotted, linear) in the overall Lebu Valley of East Himalayas.

demonstrates that THg in soil and THg in small mammals both followed a hump-shaped pattern–better fitted by a quadratic (order 2) or cubic (order 3) equation of elevation than a linear equation, while the mammal species richness generally decreased monotonically along elevation–better fitted by a linear (order 1) equation (Table 1, Fig. 2). Specifically, the low/middle elevation in both soil and hair THg were significantly higher than the high elevation (Chi-squared = 27.62, df = 2, p-value <0.001 for soil THg, while chi-squared = 9.62, df = 2, p-value = 0.008 for hair THg), however no significant difference existed between low and middle elevations. In details (Fig. 2), soil THg reached a peak at about 3200 m a.s.l. of coniferous and broadleaf mixed forest, while hair THg elevated in 3500–3800 m a.s.l. of the dark coniferous forested zone. The THg trends we observed in topsoil and small mammals suggest that at extremely high altitudes, Hg contamination may not simply follow the "mountain cold-trapping effect".

In the meantime, our survey also identified the distribution of mammal species in this valley (Fig. 3). Specifically, 21 and 15 species were found at low and mid elevation bands respectively, whereas only 6 species had a distribution at high elevation bands i. e > 4100 m a.s.l. Notably, according to IUCN Red List (https://www.iucn.org/redlist), 10 of 10 threaten species such as Asia golden cat *Catopuma temminckii* and Leopard *Panthera pardus* inhabit at low and mid-elevations, while only 1 of 10 threaten species, the Black Musk Deer *Moschus fuscus* found at extremely high altitudes. Although we were not able to collect related samples from the higher trophic position, likely, the Hg risk to top avian and mammalian predators might already occur if there are multiple steps in Hg accumulation (Lavoie et al., 2013). In addition, small mammals at low-and mid-elevations might be exposed to elevated MeHg bioaccumulation in the Himalayas indicated by elevated hair THg, since MeHg is assumed to be the predominant form of Hg in hair of mammals (Evans et al., 2000; Wang et al., 2014). Unfortunately, species richness

Table 1
Polynomial regression analyses were performed to assess the form of the elevational patterns of THg (both in soil and small mammals) as a function of elevation along the gradient. All polynomial regressions are significant (P < 0.05). Bold numbers indicate the best regression model selected by the lowest Akaike information criterion value (AICc).

	Order 1	Order 2	Order 3
	AICc	AICc	AICc
Soil THg	417.563	400.650	**378.833**
Hair THg	681.574	**677.953**	680.261
Species richness	**29.556**	33.778	33.680

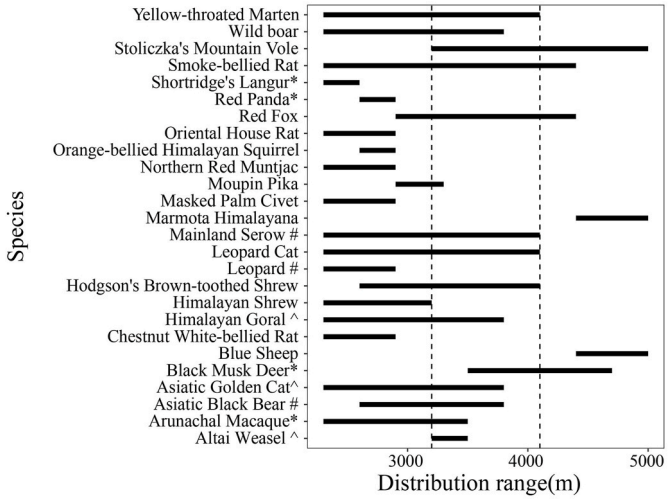

Fig. 3. The elevational ranges of non-volant mammal species in the Lebu Valley. Symbol *: endangered species; #: vulnerable species; ^: Near Threatened species (IUCN Red List). The dash lines indicated the boundaries between low and middle (3200 m a.s.l.), middle and high (4100 m a.s.l.) elevational ranges. For visualization, species scientific names are shown in Table S1.

and Hg concentration all found elevated at low and middle elevations, suggesting possibly that enhanced Hg exposure might exist in top predatory species in this range. In fact, similar to the widely reported hump-shaped pattern found in species richness in mountain systems along elevational gradients (McCain, 2009, 2007; 2005; Rahbek, 1995), the highest biodiversity of reptiles (Chettri et al., 2010), birds (Acharya et al., 2011; Hu et al., 2018; Pan et al., 2016) and mammals (Hu et al., 2017, 2018) frequently appears at low-mid elevations in the Himalayas. Thus, our findings shed light to the concerns in ecological conservation of fragile biodiversity in the Himalayan Mountains.

3.2. Environmental factors influencing soil Hg contamination

The details of vegetation type, NDVI, SOM, temperature and precipitation can be found in Table S3. Based on our model selection, there is only 1 of eleven candidate models within △AIC*c* less than 2 (Table 2). According to the best linear model, the predictors vegetation type as well as SOM together, explained 75.65% of soil THg ($P < 0.0001$). Furthermore, both variable importance and the number of containing models (Table S4) indicated that vegetation and SOM are the most important predictors (weight = 1.00), while temperature, precipitation and NDVI are less influencing factors (all have weight less than 0.01). The second-best model that included vegetation only, resulting in a decrease in △AIC*c* greater than 19, and model weight w_i equal to 0.00, indicating the unparallel importance of the combination of vegetation and SOM in predicting soil THg (Table 2).

In remote high-altitude areas, multiple drivers complicatedly contribute to Hg accumulation. Among them, forests are important receptors for atmospheric Hg deposition (Graydon et al., 2009) and vegetation type is known as an important factor influencing the biogeochemical cycle of Hg in terrestrial ecosystems (Obrist et al., 2012). In addition, Gerson et al. (2017) highlighted elevation as well as forest type both contributed to soil Hg. Our models support the recent findings (Xue et al., 2019), further pointing out that the SOM plays an essential role in Hg accumulation along terrestrial landscapes. This is likely due to the strong binding affinity between Hg and thiol (-SH) groups in organic matter (Skyllberg et al., 2000). Other factors, such as precipitation, which is able to facilitate vegetation growth, might also contribute to Hg in soil via complicated interactions on biomass production and litter decomposition processes (Wang et al., 2019), but had little influence when compared with strong influencing factors (i.e. vegetation type as well as SOM) as stated by our models.

3.3. Predictors of small mammalian Hg

Small mammals serve as the base of the energy flow for predatory species in the entire food webs. When considering factors to predict THg biocontamination, there are 3 of 15 candidate models within △AIC*c* less than 2 (Table 3). The soil THg explained most of the variation in hair THg (wi = 0.29). Notably, variable importance and the number of containing models (Table S5) also indicated that the habitat i.e. vegetation type is an important factor (sum of weight: 0.66, 8 models contained), followed by soil THg (sum of weight: 0.5, 2 models contained), then SOM (sum of weight: 0.41, 6 models contained). Other factors such as precipitation, temperature and NDVI are less likely to influence THg in small mammals. The second-best model that includes both soil THg and SOM resulted in a decrease in △AIC*c* to 0.4 and slightly lower model weight ($w_i = 0.24$) (Table 3), while the third alternative model including both soil THg and vegetation resulted in a drop of △AICc to 0.6 and weight to 0.21.

The best linear regression model including only soil THg explains 11.31% of hair THg ($P < 0.0001$), suggests the complexity of Hg transportation along food webs and less predictable by a single factor i.e., soil THg here. Diet structure possibly is a strong factor when considering Hg bioaccumulation (Peterson et al., 2021). Here, we measured 6 individuals belong to Soriculus, which primary forage on invertebrates. Even within a small sample size, 2 of 6 invertebrate-eating individuals (8306.5 and 1415.0 μg/kg Hg) exceed the contamination threshold for non-human mammals at 1100 μg/kg Hg in hair (Suzuki,

Table 2
Model selection for predicting soil THg collected in the Lebu Valley of East Himalayas.

Model	K	logLik	AICc	ΔAICc	Weight
Soil THg ~ SOM + vegetation	7	¬15.64	48.39	0	1.00
Soil THg ~ vegetation	6	¬26.76	67.79	19.41	0.00
Soil THg ~ vegetation + precipitation	7	¬26.12	69.36	20.97	0.00
Soil THg ~ vegetation + temperature	7	¬26.19	69.5	21.11	0.00
Soil THg ~ NDVI + vegetation	7	¬26.54	70.19	21.8	0.00
Soil THg ~ SOM + temperature	4	¬31.35	71.73	23.34	0.00
Soil THg ~ SOM + precipitation	4	¬32.87	74.77	26.38	0.00
Soil THg ~ temperature	3	¬38.96	84.52	36.13	0.00
Soil THg ~ NDVI	3	¬39.18	84.96	36.57	0.00
Soil THg ~ precipitation	3	¬40.84	88.27	39.89	0.00
Soil THg ~ SOM	3	¬42.27	91.15	42.76	0.00

Table 3
Model selection for predicting hair THg collected at East Himalayas in 2019 summer.

Model	K	logLik	AICc	ΔAICc	weight
Hair THg ~ Soil THg	3	64.89	136.15	0	0.29
Hair THg ~ vegetation + SOM	7	60.34	136.55	0.4	0.24
Hair THg ~ vegetation + Soil THg	7	60.44	136.75	0.6	0.21
Hair THg ~ temperature + SOM + vegetation	8	60.28	139	2.85	0.07
Hair THg ~ precipitation + SOM + vegetation	8	60.3	139.05	2.9	0.07
Hair THg ~ vegetation	6	63.69	140.76	4.61	0.03
Hair THg ~ vegetation + precipitation	7	62.62	141.1	4.95	0.02
Hair THg ~ SOM	3	67.54	141.45	5.3	0.02
Hair THg ~ precipitation + SOM	4	67.22	143.08	6.93	0.01
Hair THg ~ vegetation + SOM	7	63.64	143.14	6.99	0.01
Hair THg ~ vegetation + temperature	7	63.69	143.24	7.09	0.01
Hair THg ~ temperature + SOM	4	67.34	143.31	7.16	0.01
Hair THg ~ NDVI	3	69.05	144.47	8.32	0
Hair THg ~ temperature	3	69.17	144.71	8.56	0
Hair THg ~ precipitation	3	69.22	144.82	8.68	0

1979). The advisory maximum tolerable level of human hair is 6000 μg/kg Hg (Lodenius et al., 1983), in this case, 1 of 6 sampled invertebrate-eating shrews is still caught concern regarding to Hg accumulation in organisms at higher trophic positions (Lavoie et al., 2013). Thus, due to the accumulation characteristics of Hg, Soriculus might have a relatively higher Hg accumulation due to diet structure. Further investigation into this family with a larger sample size is needed.

4. Conclusions and future research

Overall, our study reveals a unique pattern of Hg accumulation along a 2700-m elevational gradient in the East Himalayas of Southwestern China. The low/middle elevation in both soil THg and hair THg were significantly higher than the high elevation area. Combined with field investigation, our findings show that the Hg risk to terrestrial mammals distributes disproportionately and overlaps species richness in mountain systems along elevational gradients. Further attention should be given to mammals inhabiting low and mid-elevational ranges. Together, our results provide strong evidence that vegetation and SOM strongly influence soil THg; while soil THg, vegetation as well as SOM contribute to the Hg accumulation in small mammals. Based on our results, temperature and precipitation predict less for THg accumulation. Taken together, our study advances the understanding of the effects of environmental and elevational factors on patterns of Hg bioaccumulation in environmental compartments as well as fauna in montane ecosystems within the extremely high altitudes in Asia.

For the active implementation of the Minamata Convention on Mercury (www.mercuryconvention.org), the development of biomonitoring program in pristine region is needed to build the baseline data for both environmental compartments and montane fauna. Particularly, measurement of contaminants in indicator organisms will provide accurate data for bioavailability, mobility and fate of environmental contaminants in this highest mountain terrestrial system. Instead of the examined factors, please note we did not test whether THg concentrations in hair differed among species, year, sex, and age class, etc. In addition, little is known about the bioaccumulation and trophic transfer of THg and particularly MeHg, via food webs in different terrestrial ecosystems along the high mountainous areas. Besides, whether this differential pattern in both surface soil and small mammals for Hg contamination among terrestrial ecosystems in other valleys of the Himalayas? Further, we only sampled in the wet season (summer). Since the Indian monsoon during the summer plays a key driver in bringing larger precipitation, while in winter, the westerly wind might reduce the amount of precipitation in the dry season, but the heating activities potentially increase the emission in the meantime, thus, the seasonal changes in Hg accumulation might exist. Moreover, as global climate warming, melting of glaciers in high mountains continuedly releases a large quantity of Hg originally locked in the ice into the atmosphere and downstream ecosystems, potentially accelerate the uptake of atmospheric Hg (Wang et al., 2020). This region is already sensitive to climate change, then Hg contamination might enhance at vegetated ecosystems e.g. the ecozone, and further influence the hotspot of biodiversity in a complicated way. The increased loads of altitudinally enhanced Hg in montane might potentially bring profound impacts. These research questions worth more attention and investigative efforts for wildlife conservation in this biodiversity hotspot of the highest mountainous region.

Declaration of competing interest

The authors declare that they have no known competing financial interests or personal relationships that could have appeared to influence the work reported in this paper.

Acknowledgement

We express our gratitude to Zuobo Wang and Qiujian Li in helping collecting samples for our study. We are also grateful to the Forestry Bureau of Cuona County for the great support of our work. Thanks to the three anonymous reviewers for providing comments that improved the manuscript. This work was financed by the National Natural Science Foundation of China (NSFC31901109); Strategic Priority Research Programs of the Chinese Academy of Sciences, the Pan-Third Pole Environment Study for a Green Silk Road (Pan-TPE, XDA20040502) and the National Natural Science Foundation of China (NSFC31901220, NSFC41877405); GDAS Project of Science and Technology Development (2019GDASYL-0105044); The Biodiversity Survey and Assessment Project of the Ministry of Ecology and Environment, China (2019HJ2096001006); GDAS Special Project of Science and Technology Development (2018GDASCX-0107); The Fellowship of China Postdoctoral Science Foundation (2020M671285).

Appendix A. Supplementary data

Supplementary data to this article can be found online at https://doi.org/10.1016/j.envpol.2021.117752.

Credit author statement

Yanju Ma: Conceptualization; Formal analysis; Sample preparation; Writing – original draft; Writing - editing; Funding acquisition. Wei Zhang: Formal analysis; Data curation; Writing - editing. Huijian Hu: Writing - editing; Field work, Funding acquisition. Lihai Shang: Resources, Writing - editing; Funding acquisition. Lianghua Chen: Resources. Zhixin Zhou: Writing - editing; Field work; Funding acquisition. Paras Singh: Writing - editing; Field work. Yiming Hu: Conceptualization, Data curation and Formal analysis, Writing – review & editing; Field work; Resources; Funding acquisition.

References

Acharya, B.K., Sanders, N.J., Vijayan, L., Chettri, B., 2011. Elevational gradients in bird diversity in the Eastern Himalaya: an evaluation of distribution patterns and their underlying mechanisms. e29097 PLoS One 6, e29097. https://doi.org/10.1371/journal.pone.0029097.

Bartoń, K., 2019. MuMIn: Multi-Model Inference. R package version 1.43.15. https://CRAN.R-project.org/package=MuMIn.

Blackwell, B.D., Driscoll, C.T., 2015. Deposition of mercury in forests along a montane elevation gradient. Environ. Sci. Technol. 49, 5363–5370. https://doi.org/10.1021/es505928w.

Blais, J.M., Charpentié, S., Pick, F., Kimpe, L.E., Amand, A.S., Regnault-Roger, C., 2006. Mercury, polybrominated diphenyl ether, organochlorine pesticide, and polychlorinated biphenyl concentrations in fish from lakes along an elevation transect in the French Pyrénées. Ecotoxicol. Environ. Saf. 63, 91–99. https://doi.org/10.1016/j.ecoenv.2005.08.008.

Burnham, K.P., Anderson, D.R., Huyvaert, K.P., 2011. AIC model selection and multimodel inference in behavioral ecology: some background, observations, and comparisons. Behav. Ecol. Sociobiol. 65, 23–35.

Chételat, J., Ackerman, J.T., Eagles-Smith, C.A., Hebert, C.E., 2020. Methylmercury exposure in wildlife: a review of the ecological and physiological processes affecting contaminant concentrations and their interpretation. Sci. Total Environ. 711, 135117. https://doi.org/10.1016/j.scitotenv.2019.135117.

Chettri, B., Bhupathy, S., Acharya, B.K., 2010. Distribution pattern of reptiles along an eastern Himalayan elevation gradient, India. Acta Oecol. 36, 16–22. https://doi.org/10.1016/j.actao.2009.09.004.

Crewther, W.G., Fraser, R.D.B., Lennox, F.G., Lindley, H., 1965. The chemistry of keratins. In: Anfinsen, C.B., Anson, M.L., Edsall, J.T., Richards, F.M. (Eds.), Advances in Protein Chemistry. Academic Press, pp. 191–346. https://doi.org/10.1016/S0065-3233(08)60390-3.

Driscoll, C.T., Mason, R.P., Chan, H.M., Jacob, D.J., Pirrone, N., 2013. Mercury as a global pollutant: sources, pathways, and effects. Environ. Sci. Technol. 47, 4967–4983. https://doi.org/10.1021/es305071v.

Ecke, F., Benskin, J.P., Berglund, Å.M.M., de Wit, C.A., Engström, E., Plassmann, M.M., Rodushkin, I., Sörlin, D., Hörnfeldt, B., 2020. Spatio-temporal variation of metals and organic contaminants in bank voles (*Myodes glareolus*). Sci. Total Environ. 713, 136353 https://doi.org/https://doi.org/10.1016/j.scitotenv.2019.136353.

Evans, R.D., Addison, E.M., Villeneuve, J.Y., MacDonald, K.S., Joachim, D.G., 2000. Distribution of inorganic and methylmercury among tissues in mink (*Mustela vison*)

and otter (*Lutra canadensis*). Environ. Res. 84, 133–139. https://doi.org/10.1006/enrs.2000.4077.
Fu, X., Zhang, H., Liu, C., Zhang, H., Lin, C.-J., Feng, X., 2019. Significant seasonal variations in isotopic composition of atmospheric total gaseous mercury at forest sites in China caused by vegetation and mercury sources. Environ. Sci. Technol. 53, 13748–13756. https://doi.org/10.1021/acs.est.9b05016.
Gdula-Argasińska, J., Appleton, J., Sawicka-Kapusta, K., Spence, B., 2004. Further investigation of the heavy metal content of the teeth of the bank vole as an exposure indicator of environmental pollution in Poland. Environ. Pollut. 131, 71–79. https://doi.org/10.1016/j.envpol.2004.02.025.
Gerson, J.R., Driscoll, C.T., Demers, J.D., Sauer, A.K., Blackwell, B.D., Montesdeoca, M. R., Shanley, J.B., Ross, D.S., 2017. Deposition of mercury in forests across a montane elevation gradient: elevational and seasonal patterns in methylmercury inputs and production. J. Geophys. Res. Biogeosciences. 122, 1922–1939. https://doi.org/10.1002/2016JG003721.
Gerstenberger, S.L., Cross, C.L., Divine, D.D., Gulmatico, M.L., Rothweiler, A.M., 2006. Assessment of mercury concentrations in small mammals collected near Las Vegas, Nevada, USA. Environ. Toxicol. 21, 583–589. https://doi.org/10.1002/tox.20221.
Graydon, J.A., Louis, V.L., Hintelmann, H., Lindberg, S.E., Sandilands, K.A., Rudd, J.W. M., Kelly, C.A., Tate, M.T., Krabbenhoft, D.P., Lehnherr, I., 2009. Investigation of uptake and retention of atmospheric Hg (II) by boreal forest plants using stable Hg isotopes. Environ. Sci. Technol. 43, 4960–4966. https://doi.org/10.1021/es900357s. St.
Huckabee, J.W., Cartan, F.O., Kennington, G.S., 1972. Environmental Influence on Trace Elements in Hair of 15 Species of Mammals. ORNLTM3747. U.S. Atomic Energy Commission, Washington, DC.
Hu, Y., Jin, K., Huang, Z., Ding, Z., Liang, J., Pan, X., Hu, H., Jiang, Z., 2017. Elevational patterns of non-volant small mammal species richness in Gyirong Valley, Central Himalaya: evaluating multiple spatial and environmental drivers. J. Biogeogr. 44, 2764–2777. https://doi.org/10.1111/jbi.13102.
Hu, Y., Liang, J., Jin, K., Ding, Z., Zhou, Z., Hu, H., Jiang, Z., 2018. The elevational patterns of mammalian richness in the Himalayas. Biodivers. Sci. 26 (2), 191–201.
Jiang, Z.G., Ma, Y., Wu, Y., Wang, Y.X., Zhou, K.Y., Liu, S.Y., Feng, Z.J. (Eds.), 2015. China's Mammal Diversity and Geographic Distribution. Science Press, Beijing.
Lavoie, R.A., Jardine, T.D., Chumchal, M.M., Kidd, K.A., Campbell, L.M., 2013. Biomagnification of mercury in aquatic food webs: a worldwide meta-analysis. Environ. Sci. Technol. 47, 13385–13394. https://doi.org/10.1021/es403103t.
Lodenius, M., Seppänen, A., Herranen, M., 1983. Accumulation of mercury in fish and man from reservoirs in Northern Finland. Water. Air. Soil Pollut. 19, 237–246. https://doi.org/10.1007/BF00599051.
Loewen, M.D., Sharma, S., Tomy, G., Wang, F., Bullock, P., Wania, F., 2005. Persistent organic pollutants and mercury in the Himalaya. Aquat. Ecosys. Health Manag. 8, 223–233. https://doi.org/10.1080/14634980500220924.
Martinková, B., Janiga, M., Pogányová, A., 2019. Mercury contamination of the snow voles (*Chionomys nivalis*) in the West Carpathians. Environ. Sci. Pollut. Res. 26, 35988–35995. https://doi.org/10.1007/s11356-019-06714-6.
McCain, C.M., 2009. Global analysis of bird elevational diversity. Global Ecol. Biogeogr. 18, 346–360. https://doi.org/10.1111/j.1466-8238.2008.00443.x.
McCain, C.M., 2007. Area and mammalian elevational diversity. Ecology 88, 76–86 https://doi.org/https://doi.org/10.1890/0012-9658(2007)88[76:AAMED]2.0.CO;2.
McCain, C.M., 2005. Elevational gradients in diversity of small mammals. Ecology 86, 366–372. https://doi.org/10.1890/03-3147.
Myers, N., Mittermeier, R.A., Mittermeier, C.G., da Fonseca, G.A., Kent, J., 2000. Biodiversity hotspots for conservation priorities. Nature 403, 853–858. https://doi.org/10.1038/35002501.
Nelson, D.W., Sommers, L.E., 1996. Total carbon, organic carbon, and organic matter. Methods Soil Anal. SSSA Book Series. https://doi.org/10.2136/sssabookser5.3.c34.
Obrist, D., Agnan, Y., Jiskra, M., Olson, C.L., Colegrove, D.P., Hueber, J., Moore, C.W., Sonke, J.E., Helmig, D., 2017. Tundra uptake of atmospheric elemental mercury drives Arctic mercury pollution. Nature 547, 201–204.
Obrist, D., Johnson, D.W., Edmonds, R.L., 2012. Effects of vegetation type on mercury concentrations and pools in two adjacent coniferous and deciduous forests. J. Plant Nutr. Soil Sci. 175, 68–77. https://doi.org/10.1002/jpln.201000415.
Oliver, M.A., Webster, R., 2007. Kriging : a method of interpolation for geographical information systems. Int. J. Geogr. Inf. Syst. 4, 313–332. https://doi.org/10.1080/02693799008941549.
Pan, X., Ding, Z., Hu, Y., Liang, J., Wu, Y., Si, X., Guo, M., Hu, H., Jin, K., 2016. Elevational pattern of bird species richness and its causes along a central Himalaya gradient, China. PeerJ 4, e2636. https://doi.org/10.7717/peerj.2636.
Pankakoski, E., Hyvärinen, H., Jalkanen, M., Koivisto, I., 1993. Accumulation of heavy metals in the mole in Finland. Environ. Pollut. 80, 9–16. https://doi.org/10.1016/0269-7491(93)90003-7.
Peterson, S.H., Ackerman, J.T., Hartman, C.A., Casazza, M.L., Feldheim, C.L., Herzog, M. P., 2021. Mercury exposure in mammalian mesopredators inhabiting a brackish marsh. Environ. Pollut. 273, 115808. https://doi.org/10.1016/j.envpol.2020.115808.
Rahbek, C., 1995. The elevational gradient of species richness: a uniform pattern? Ecography 18, 200–205. https://doi.org/10.1111/j.1600-0587.1995.tb00341.x.
Rice, K.M., Walker, E.M., Wu, M., Gillette, C., Blough, E.R., 2014. Environmental mercury and its toxic effects. J. Prev. Med. Public Heal. 47, 74–83. https://doi.org/10.3961/jpmph.2014.47.2.74.
Skyllberg, U., Xia, K., Bloom, P.R., Nater, E.A., Bleam, W.F., 2000. Binding of mercury (II) to reduced sulfur in soil organic matter along upland-peat soil transects. J. Environ. Qual. 29, 855–865. https://doi.org/10.2134/jeq2000.00472425002900030022x.
Stankwitz, C., Kaste, J.M., Friedland, A.J., 2012. Threshold increases in soil lead and mercury from tropospheric deposition across an elevational gradient. Environ. Sci. Technol. 46, 8061–8068. https://doi.org/10.1021/es204208w.
Sun, X., Zhang, Q., Li, M., Kandel, K., Rawat, B., Pandey, A., Guo, J., Kang, S., Pant, R.R., Cong, Z., Zhang, F., 2020. Mercury variation and export in trans-Himalayan rivers: insights from field observations in the Koshi River. Sci. Total Environ. 738, 139836. https://doi.org/10.1016/j.scitotenv.2020.139836.
Suzuki, T., 1979. Dose-effect and dose-response relationships of mercury and its derivatives. In: Nriagu, J.O. (Ed.), The Biogeochemistry of Mercury in the Environment. Elsevier/North-Holland Biomedical Press, New York, pp. 399–431.
Symonds, M.R.E., Moussalli, A., 2011. A brief guide to model selection, multimodel inference and model averaging in behavioural ecology using Akaike's information criterion. Behav. Ecol. Sociobiol. 65, 13–21. https://doi.org/10.1007/s00265-010-1037-6.
Talmage, S.S., Walton, B.T., 1991. Small mammals as monitors of environmental contaminants. In: Ware, G.W. (Ed.), Reviews of Environmental Contamination and Toxicology. Springer New York, New York, pp. 47–145. https://doi.org/10.1007/978-1-4612-3078-6_2.
Townsend, J.M., Driscoll, C.T., Rimmer, C.C., McFarland, K.P., 2014. Avian, salamander, and forest floor mercury concentrations increase with elevation in a terrestrial ecosystem. Environ. Toxicol. Chem. 33, 208–215.
Tripathee, L., Guo, J., Kang, S., Paudyal, R., Sharma, C.M., Zhang, Q., Rupakheti, D., Ghimire, P.S., Gyawali, A., 2019. Assessments of mercury along the elevation gradient in soils of Langtang. Hum. Ecol. Risk Assess. 25, 1006–1017. https://doi.org/10.1080/10807039.2018.1459180.
Turna Demir, F., Yavuz, M., 2020. Heavy metal accumulation and genotoxic effects in levant vole (*Microtus guentheri*) collected from contaminated areas due to mining activities. Environ. Pollut. 256, 113378. https://doi.org/10.1016/j.envpol.2019.113378.
UN Environment, 2019. Global Mercury Assessment 2018, UN Environment Programme. Chemicals and Health Branch Geneva, Switzerland.
U.S. Environmental Protection Agency, 2000. Method 7473, Mercury in Solids and Solutions by Thermal Decomposition, Amalgamation, and Atomic Absorption Spectrophotometry. Test Methods for Evaluating Solid Waste, Physical/chemical Methods; SW 846, Update IVA. U.S. Government printing office, Washington, D.C.
Wang, W., Evans, R.D., Hickie, B.E., Rouvinen-Watt, K., Evans, H.E., 2014. Methylmercury accumulation and elimination in mink (*Neovison vison*) hair and blood: results of a controlled feeding experiment using stable isotope tracers. Environ. Toxicol. Chem. 33, 2873–2880. https://doi.org/10.1002/etc.2762.
Wang, X., Luo, J., Yuan, W., Lin, C.J., Wang, F., Liu, C., Wang, G., Feng, X., 2020. Global warming accelerates uptake of atmospheric mercury in regions experiencing glacier retreat. Proc. Natl. Acad. Sci. Unit. States Am. 117, 2049–2055. https://doi.org/10.1073/pnas.1906930117.
Wang, X., Yuan, W., Lu, Z., Lin, C.J., Yin, R., Li, F., Feng, X., 2019. Effects of precipitation on mercury accumulation on subtropical montane forest floor: implications on climate forcing. J. Geophys. Res. Biogeosciences 124, 959–972. https://doi.org/10.1029/2018JG004809.
Wang, X.P., Yao, T.D., Wang, P.L., Wei-Yang, Tian, L. De, 2008. The recent deposition of persistent organic pollutants and mercury to the Dasuopu glacier, Mt. Xixiabangma, central Himalayas. Sci. Total Environ. 394, 134–143. https://doi.org/10.1016/j.scitotenv.2008.01.016.
Wania, F., Mackay, D., 1995. A global distribution model for persistent organic chemicals. Sci. Total Environ. 160–161, 211–232. https://doi.org/10.1016/0048-9697(95)04358-8.
Xue, W., Kwon, S.Y., Grasby, S.E., Sunderland, E.M., Pan, X., Sun, R., Zhou, T., Yan, H., Yin, R., 2019. Anthropogenic influences on mercury in Chinese soil and sediment revealed by relationships with total organic carbon. Environ. Pollut. 255, 1. https://doi.org/10.1016/j.envpol.2019.113186.
Yu, X., Driscoll, C.T., Montesdeoca, M., Evers, D., Duron, M., Williams, K., Schoch, N., Kamman, N.C., 2011. Spatial patterns of mercury in biota of Adirondack, New York lakes. Ecotoxicology 20, 1543–1554. https://doi.org/10.1007/s10646-011-0717-y.
Zhang, H., Yin, R.S., Feng, X. Bin, Sommar, J., Anderson, C.W.N., Sapkota, A., Fu, X.W., Larssen, T., 2013. Atmospheric mercury inputs in montane soils increase with elevation: evidence from mercury isotope signatures. Sci. Rep. 3, 1–8. https://doi.org/10.1038/srep03322.